Hindawi Publishing Corporation
Journal of Nanomaterials
Volume 2012, Article ID 594290, 5 pages
doi:10.1155/2012/594290

Research Article

Propeller-Shaped ZnO Nanostructures Obtained by Chemical Vapor Deposition: Photoluminescence and Photocatalytic Properties

S. L. Wang,[1] H. W. Zhu,[1] W. H. Tang,[2] and P. G. Li[1]

[1] *Department of Physics, Zhejiang Sci-Tech University, Hangzhou 310018, China*
[2] *School of Science, Beijing University of Posts and Telecommunications, Beijing 100876, China*

Correspondence should be addressed to S. L. Wang, slwang@zstu.edu.cn and P. G. Li, pgli@zstu.edu.cn

Received 30 September 2011; Revised 16 November 2011; Accepted 25 November 2011

Academic Editor: Laécio Santos Cavalcante

Propeller-shaped and flower-shaped ZnO nanostructures on Si substrates were prepared by a one-step chemical vapor deposition technique. The propeller-shaped ZnO nanostructure consists of a set of axial nanorod (50 nm in tip, 80 nm in root and 1 μm in length), surrounded by radial-oriented nanoribbons (20–30 nm in thickness and 1.5 μm in length). The morphology of flower-shaped ZnO nanostructure is similar to that of propeller-shaped ZnO, except the shape of leaves. These nanorods leaves (30 nm in diameter and 1–1.5 μm in length) are aligned in a radial way and pointed toward a common center. The flower-shaped ZnO nanostructures show sharper and stronger UV emission at 378 nm than the propeller-shaped ZnO, indicating a better crystal quality and fewer structural defects in flower-shaped ZnO. In comparison with flower-shaped ZnO nanostructures, the propeller-shaped ZnO nanostructures exhibited a higher photocatalytic property for the photocatalytic degradation of Rhodamine B under UV-light illumination.

1. Introduction

Zinc oxide (ZnO), a remarkable II–VI semiconductor with a wide direct band gap of 3.37 eV and large exciton binding energy of 60 meV at room temperature, has attracted considerable interests due to potential application in photocatalysis [1], sensors [2], light-emitting diodes [3], solar cells [4], and so forth. Compared with TiO_2, ZnO as a potential photocatalyst has the advantage of lower cost, absorbing more light quanta and higher photocatalytic efficiencies for the degradation of several organic pollutants in both acidic and basic medium than TiO_2 [5, 6]. Many strategies have been developed to improve the photocatalytic activity of ZnO nanostructures such as changing the structural and morphological characters (size, shape, and crystalline structure, etc.) [7, 8]. A variety of ZnO nanostructures such as nanowires [9], nanorings [10], nanorods [11], nanobelts [12], nanosheets [13], and star-shaped nanostructures [14] have been synthesized by a number of techniques, which mainly include the hydrothermal synthesis [15], solution-based synthesis [16], template-based synthesis [17], chemical vapor deposition (CVD) [18], arc discharge technique [19], and thermal evaporation process [20]. Although many works have been reported about the ZnO nanostructures, little information concerning the photocatalytic activity of propeller-shaped ZnO nanostructures was presented in previous studies [21, 22].

In this letter, propeller-shaped and flower-shaped ZnO nanostructures were prepared on Si substrates by a one-step chemical vapor deposition technique. The morphology, crystal structure, optical property, and photocatalytic property were studied.

2. Experimental Section

2.1. Sample Preparation. N type Si (001) substrates (1.5 cm × 1.5 cm) were ultrasonically cleaned in hydrochloric acid solution, acetone, and deionized water for 30 min, respectively. Commercial Zn powder (1.0 g) with a purity of 99.999% was used as the source material and put in an alumina boat, two pieces of Si substrates (position1: near the Zn powder at a

distance of 3 cm, the sample was labeled as S1; position 2: far from the Zn powder at a distance of 5 cm, the sample was labeled S2) were placed sequentially in the alumina boat. The boat was loaded into a furnace with a horizontal alumina tube. Two ends of the tube were sealed using mechanically clamped steel plates with the rubber gaskets. The tube was evacuated by a mechanical rotary pump. Then the furnace temperature was raised to 1000°C at a rate of ~20°C/min while oxygen gas was introduced into the chamber. After reaction for 1 h, the furnace was cooled down to room temperature naturally.

2.2. Characterization. The crystallographic information of the prepared samples was analyzed by powder X-ray diffraction (XRD) using a Bruker AXS D8 DISCOVER X-ray diffractometer with Cu Kα radiation ($\lambda = 1.5406$ Å). The morphology and composition of the as-deposited products were characterized by field emission scanning electron microscope (FESEM, S-4800) and energy-dispersive X-ray spectrometry (EDX), respectively. Transmission electron microscopy (TEM) and high-resolution transmission electron microscopy (HRTEM) were performed on JEOL 2010F high-resolution TEM system. Photoluminescence properties of ZnO nanostructures were measured on a FLSP920 fluorescence spectrometer using a Xe lamp with the excitation wavelength of 320 nm at room temperature. Brunauer-Emmett-Teller (BET) nitrogen adsorption-desorption was measured using a Micromeritics ASAP 2010 system.

The photocatalytic activity of the prepared samples was evaluated by the photocatalytic degradation of RhB aqueous solution performed at room temperature (ca. 20°C). The experimental procedure was as follows. 0.01 g of the prepared powders was dispersed in 30 mL of RhB aqueous solution with a concentration of 1.0×10^{-5} mol·L^{-1} in a beaker (with a capacity of 50 mL), and the suspensions were placed in dark for 30 min before illumination to allow sufficient adsorption of RhB. A 100 W mercury lamp placed 2 cm above the beaker with a wavelength of 365 nm was used as a light source. The concentration of RhB aqueous solution was determined by a UV-visible spectrophotometer (UV-4802H, UNICO). After UV-light irradiation for 30 min, the reaction solution was filtered, and then the absorbance of RhB aqueous solution was measured.

3. Results and Discussion

XRD analysis was adopted to analyze the crystal structure and phase composition of the obtained products. Figures 1(a, b) show the XRD patterns of the products obtained at different position. All the diffraction peaks can be indexed to wurtzite hexagonal ZnO (JCPDS Card file no. 70-2551). No other diffraction peaks are detected, indicating that all the as-prepared products are pure ZnO. Figure 2 shows FESEM images of the products obtained at different positions. As shown in Figure 2(a), the morphology of sample S1 is similar to the propellers, which consists of a set of axial nanorod (50 nm in tip, 80 nm in root and 1 μm in length), surrounded by radial oriented nanoribbons (20–30 nm in thickness and 1.5 μm in length). Figure 2(b) shows FESEM image of sample S2. The flower-shaped products are composed of aligned nanorods (30 nm in diameter and 1–1.5 μm in length) in a radial way, and all the nanorods pointed toward a common center. BET surface area measurements of samples indicate that the S_{BET} of propeller-shaped and flower-shaped ZnO nanostructures are 23.5 m^2/g and 25.1 m^2/g, respectively.

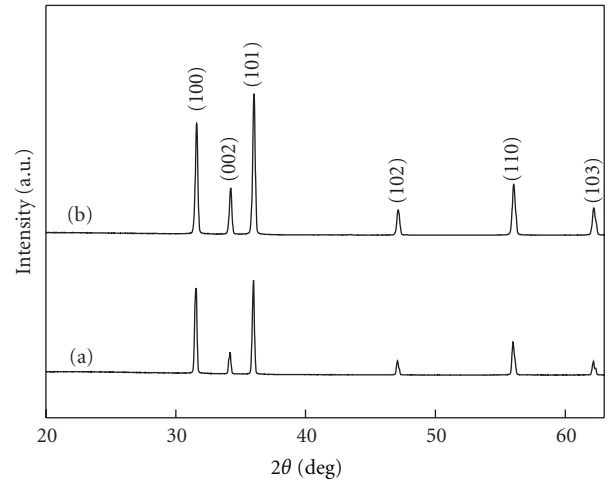

Figure 1: XRD patterns of the products obtained at different positions: (a) S1 and (b) S2.

TEM, HRTEM, and EDX were also used to characterize the structural properties of ZnO nanostructures. Figure 3(a) shows TEM image of a single nanoribbon in propeller-shaped ZnO nanostructures. The corresponding HRTEM image recorded from an individual nanoribbon (Figure 3(b)) clearly shows the well-resolved interference lattice fringe of about 0.28 nm that corresponds to the (100) crystal plane of ZnO phase. The EDX spectrum of propeller-shaped ZnO nanostructures was presented in Figure 3(c), in which the propeller-shaped products are composed only of Zn and O, and this result is in good accordance with the XRD analysis. The appearance of Si peak in the spectrum attributes to the silicon substrate. Figures 3(d), 3(e), and 3(f) show the TEM image, HRTEM image, and EDX spectrum of flower-shaped ZnO nanostructures, respectively. All character results indicate that the products synthesized in both positions are ZnO.

Figure 4 shows the room-temperature PL spectra recorded from propeller-shaped and flower-shaped ZnO nanostructures. The sharp peak at 378 nm corresponds to the near-band-edge emission (UV emission) of ZnO, which is attributed to the recombination of photogenerated electrons and holes [23]. The peak at 495 nm corresponded to the deep-level emission (visible emission) is associated with defects in ZnO lattice, such as oxygen vacancy and Zn interstitials [23, 24]. The deep-level emission (Figure 4(a), propeller-shaped ZnO) may indicate the existence of oxygen vacancies in the propeller-shaped nanostructures. Figure 4(b) shows a strong, dominated- and high-intensity peak at 378 nm in the UV region and a suppressed and weak band at 495 nm in the visible region. It is known

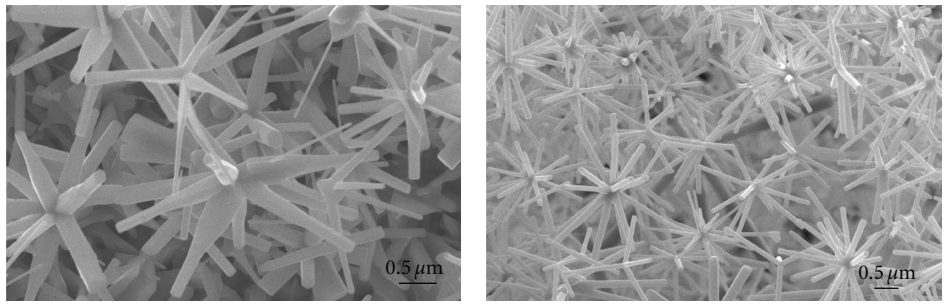

(a) (b)

Figure 2: FESEM images of (a) propeller-shaped and (b) flower-shaped ZnO nanostructures.

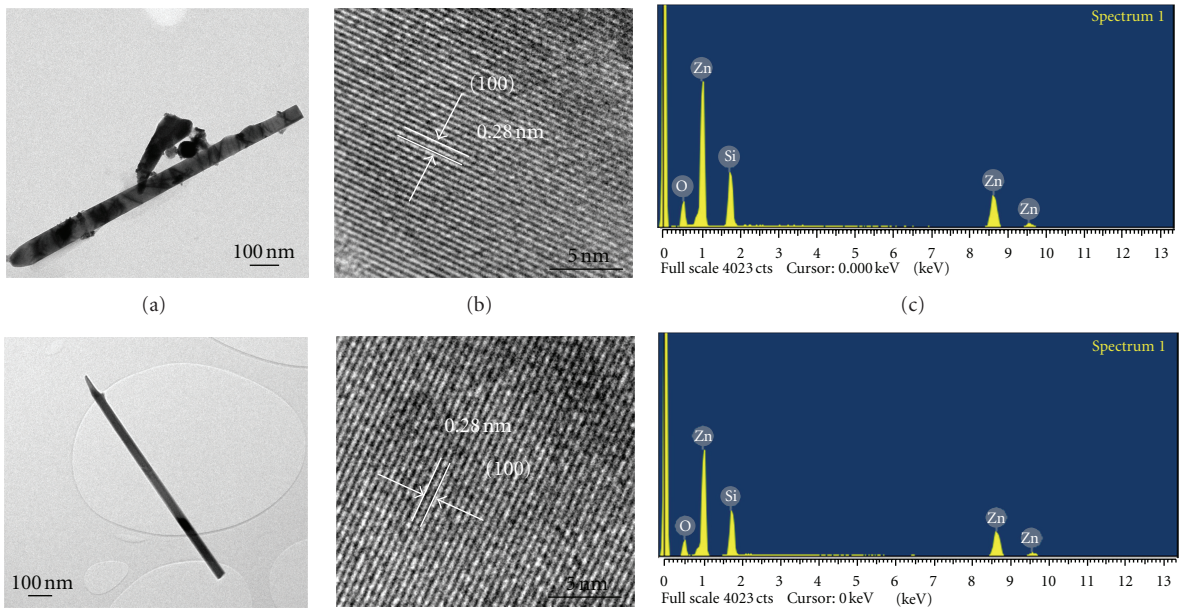

(a) (b) (c)

(d) (e) (f)

Figure 3: (a, b, and c) TEM image, HRTEM image, and EDX spectrum of the propeller-shaped ZnO nanostructures, respectively; (d, e, and f) TEM image, HRTEM image, and EDX spectrum of the flower-shaped ZnO nanostructures, respectively.

that the improvement in the crystal quality such as low-structural defects, oxygen vacancies, zinc interstitials- and decrease in the impurities may cause the appearance of sharper and stronger UV emission and a suppressed and weakened green emission [25]. Thus, the strong UV emission and weak green emission observed in Figure 4(b) (flower-shaped ZnO) may be ascribed to the good crystal quality with less structural defects of flower-shaped ZnO nanostructures. The significant defect-related emission property of ZnO nanostructures may be beneficial to their photocatalytic property.

Heterogeneous semiconductor (TiO_2 and ZnO) photocatalysis is a promising new alternative method among advanced oxidation processes (AOPs) which generally includes UV/H_2O_2, UV/O_3 or UV/Fenton's reagent for oxidative removal of organic chemicals [26–28]. To demonstrate the photocatalytic of the ZnO nanostructures, the degradation of RhB was examined as a model reaction. The variety of characteristic absorption of RhB at 554 nm was applied to monitor the photocatalytic degradation process. Figure 5 shows the UV-vis absorption spectrum of an aqueous solution of RhB (initial concentration: 1.0×10^{-5} M, 30 mL) in the presence of propeller-shaped ZnO nanostructures (0.01 g) under UV irradiation. The absorption peaks corresponding to RhB diminished gradually as the exposure time was extended. Figure 6 shows the comparison of photocatalytic activities of propeller-shaped and flower-shaped ZnO nanostructures. Significantly, the concentration of RhB barely changed without any catalyst (Figure 6(a)), whereas that of RhB gradually decreased in the presence of propeller-shaped and flower-shaped ZnO nanostructures under UV-light illumination. Obviously, the photocatalytic ability of propeller-shaped ZnO nanostructures is better than that of flower-shaped ZnO nanostructures (Figure 6(b, c)).

When the heterogeneous semiconductors are illuminated with UV-light, the electron/hole pairs are produced with

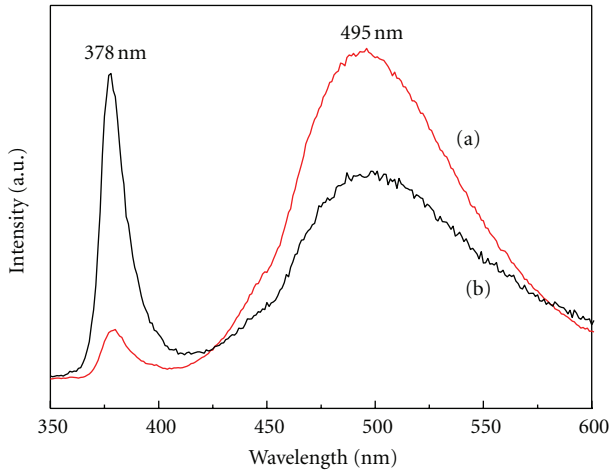

Figure 4: Photoluminescence spectra of (a) propeller-shaped and (b) flower-shaped ZnO nanostructures.

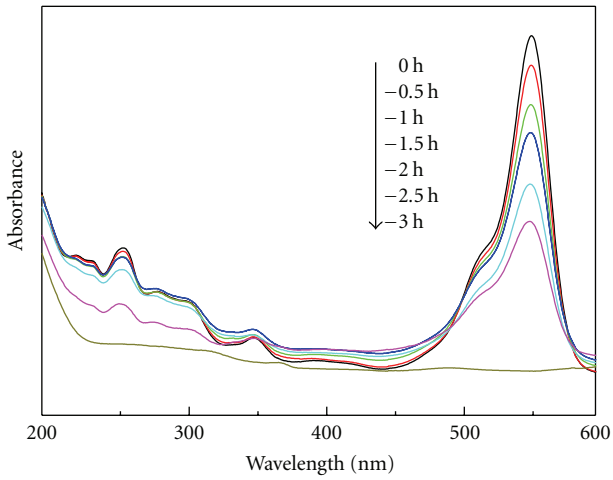

Figure 5: Absorption spectrum of the RhB solution in the presence of propeller-shaped ZnO nanostructures.

electrons promoted to the conduction band and leaving the positive holes in the valence band. These electron hole pairs can either recombine or can interact separately with other molecules and induce a complex series of reactions that might result in the complete degradation of the dye pollutants adsorbed on the surface of the semiconductor materials [29–31]. Based on the PL results mentioned above, the peak at 378 nm is due to the recombination of a photogenerated hole with an electron occupying the oxygen vacancies in the ZnO nanostructures, whereas the peak at 495 nm is caused by the recombination of electrons in single-occupied oxygen vacancies [31]. The low PL spectrum intensity at 378 nm (Figure 4(a), propeller-shaped ZnO) indicates that the rate of the recombination between photogenerated holes and electrons might be lower on the surface of propeller-shaped ZnO nanostructures than that of flower-shaped ZnO nanostructures, which is beneficial for the photocatalytic reaction. The PL spectra at 495 nm show that oxygen vacancies might

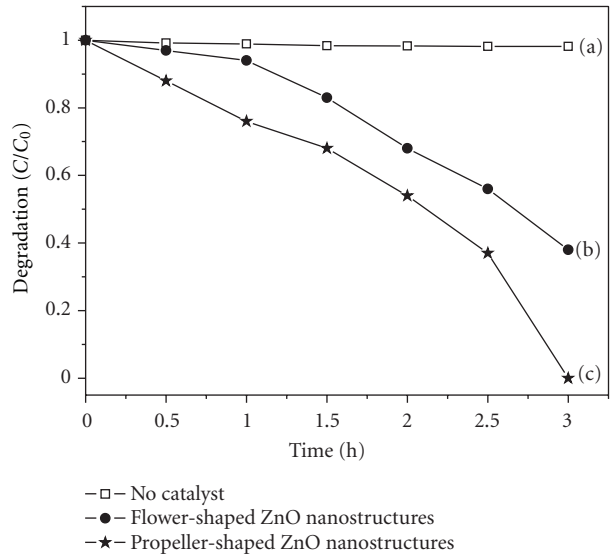

Figure 6: Photodegradation of RhB (1.0×10^{-5} M, 30 mL) under UV-light: (a) no catalyst, (b) flower-shaped ZnO nanostructures, and (c) propeller-shaped ZnO nanostructures. C is the concentration of RhB, and C_0 is the initial concentration.

be presented in both the propeller-shaped and flower-shaped ZnO nanostructures. Considering the S_{BET} of propeller-shaped samples (23.5 m^2/g) is lower than that of the flower-shaped ones (25.1 m^2/g), the higher photocatalytic property of propeller-shaped ZnO nanostructures for the degradation of RhB molecules may be caused by the lower rate of recombination between photogenerated holes and electrons on the surface of propeller-shaped ZnO nanostructures.

4. Conclusions

Propeller-shaped and flower-shaped ZnO nanostructures were prepared on Si substrates by chemical vapor deposition technique. In comparison with the propeller-shaped ZnO, the flower-shaped ZnO nanostructures show sharper and stronger UV emission at 378 nm and broader and weaker green emission at 495 nm, indicating a better crystal quality and fewer structural defects in the flower-shaped ZnO. However, the propeller-shaped ZnO nanostructures exhibited a more effective photocatalytic property for the photocatalytic degradation of Rhodamine B under UV-light illumination than flower-shaped ZnO nanostructures.

Acknowledgments

This work was supported by the National Basic Research Program of China (973 Program) (Grant no. 2010CB933501), the National Natural Science Foundation of China (Grant no. 51072182, 60806045 and 51172208), and the Natural Science Foundation of Zhejiang Province (Grant no. Y1110519).

References

[1] T. J. Kuo, C. N. Lin, C. L. Kuo, and M. H. Huang, "Growth of ultralong ZnO nanowires on silicon substrates by vapor transport and their use as recyclable photocatalysts," *Chemistry of Materials*, vol. 19, no. 21, pp. 5143–5147, 2007.

[2] X. Wang, J. Zhou, J. Song, J. Liu, N. Xu, and Z. L. Wang, "Piezoelectric field effect transistor and nanoforce sensor based on a single ZnO nanowire," *Nano Letters*, vol. 6, no. 12, pp. 2768–2772, 2006.

[3] K. Keem, D. Y. Jeong, S. Kim et al., "Fabrication and device characterization of omega-shaped-gate ZnO nanowire field-effect transistors," *Nano Letters*, vol. 6, no. 7, pp. 1454–1458, 2006.

[4] T. P. Chou, Q. Zhang, G. E. Fryxell, and G. Cao, "Hierarchically structured ZnO film for dye-sensitized solar cells with enhanced energy conversion efficiency," *Advanced Materials*, vol. 19, no. 18, pp. 2588–2592, 2007.

[5] L. Y. Yang, S. Y. Dong, J. H. Sun, J. L. Feng, Q. H. Wu, and S. P. Sun, "Microwave-assisted preparation, characterization and photocatalytic properties of a dumbbell-shaped ZnO photocatalyst," *Journal of Hazardous Materials*, vol. 179, no. 1–3, pp. 438–443, 2010.

[6] J. C. Lee, S. Park, H. J. Park, J. H. Lee, H. S. Kim, and Y. J. Chung, "Photocatalytic degradation of TOC from aqueous phenol solution using solution combusted ZnO nanopowders," *Journal of Electroceramics*, vol. 22, no. 1–3, pp. 110–113, 2009.

[7] Y. Zhang, W. Zhang, and H. Zheng, "Fabrication and photoluminescence properties of ZnO:Zn hollow microspheres," *Scripta Materialia*, vol. 57, no. 4, pp. 313–316, 2007.

[8] M. S. Mohajerani, M. Mazloumi, A. Lak, A. Kajbafvala, S. Zanganeh, and S. K. Sadrnezhaad, "Self-assembled zinc oxide nanostructures via a rapid microwave-assisted route," *Journal of Crystal Growth*, vol. 310, no. 15, pp. 3621–3625, 2008.

[9] Y. C. Kong, D. P. Yu, B. Zhang, W. Fang, and S. Q. Feng, "Ultraviolet-emitting ZnO nanowires synthesized by a physical vapor deposition approach," *Applied Physics Letters*, vol. 78, no. 4, pp. 407–409, 2001.

[10] X. Y. Kong, Y. Ding, R. Yang, and Z. L. Wang, "Single-crystal nanorings formed by epitaxial self-coiling of polar nanobelts," *Science*, vol. 303, no. 5662, pp. 1348–1351, 2004.

[11] F. P. Albores, F. P. Delgado, W. A. Flores, P. A. Madrid, E. R. Valdovinos, and M. M. Yoshida, "Microstructural study of ZnO nano structures by rietveld analysis," *Journal of Nanomaterials*, vol. 2011, Article ID 643126, 11 pages, 2011.

[12] C. Ronning, P. X. Gao, Y. Ding, Z. L. Wang, and D. Schwen, "Manganese-doped ZnO nanobelts for spintronics," *Applied Physics Letters*, vol. 84, no. 5, pp. 783–785, 2004.

[13] R. C. Wang, C. P. Liu, J. L. Huang, and S. J. Chen, "ZnO symmetric nanosheets integrated with nanowalls," *Applied Physics Letters*, vol. 87, no. 5, Article ID 053103, 2005.

[14] A. Umar, S. Lee, Y. S. Lee, K. S. Nahm, and Y. B. Hahn, "Star-shaped ZnO nanostructures on silicon by cyclic feeding chemical vapor deposition," *Journal of Crystal Growth*, vol. 277, no. 1–4, pp. 479–484, 2005.

[15] G. Amin, M. H. Asif, A. Zainelabdin, S. Zaman, O. Nur, and M. Willander, "Influence of pH, precursor concentration, growth time, and temperature on the morphology of ZnO nanostructures grown by the hydrothermal method," *Journal of Nanomaterials*, vol. 2011, Article ID 269692, 9 pages, 2011.

[16] L. Poul, S. Ammar, N. Jouini, F. Fiévet, and F. Villain, "Metastable solid solutions in the system ZnO-CoO: synthesis by hydrolysis in polyol medium and study of the morphological characteristics," *Solid State Sciences*, vol. 3, no. 1-2, pp. 31–42, 2001.

[17] X. Sun, J. Liu, and Y. Li, "Use of carbonaceous polysaccharide microspheres as templates for fabricating metal oxide hollow spheres," *Chemistry—A European Journal*, vol. 12, no. 7, pp. 2039–2047, 2006.

[18] Z. Fan, D. Wang, P. C. Chang, W. Y. Tseng, and J. G. Lu, "ZnO nanowire field-effect transistor and oxygen sensing property," *Applied Physics Letters*, vol. 85, no. 24, pp. 5923–5925, 2004.

[19] Y. C. Choi, W. S. Kim, Y. S. Park et al., "Catalytic growth of β-Ga_2O_3 nanowires by arc discharge," *Advanced Materials*, vol. 12, no. 10, pp. 746–750, 2000.

[20] D. Peng, Y. Huang, K. Yu, L. Li, and Z. Zhu, "Synthesis and field emission properties of hierarchical ZnO nanostructures," *Journal of Nanomaterials*, vol. 2010, Article ID 560409, 5 pages, 2010.

[21] J. Liu, X. Huang, Y. Li, Q. Zhong, and L. Ren, "Preparation and photoluminescence of ZnO complex structures with controlled morphology," *Materials Letters*, vol. 60, no. 11, pp. 1354–1359, 2006.

[22] Z. L. Wang, "Novel nanostructures of ZnO for nanoscale photonics, optoelectronics, piezoelectricity, and sensing," *Applied Physics A*, vol. 88, no. 1, pp. 7–15, 2007.

[23] L. Xu, Y. Guo, Q. Liao, J. Zhang, and D. Xu, "Morphological control of ZnO nanostructures by electrodeposition," *Journal of Physical Chemistry B*, vol. 109, no. 28, pp. 13519–13522, 2005.

[24] C. C. Lin, K. H. Liu, and S. Y. Chen, "Growth and characterization of Zn-ZnO core-shell polygon prismatic nanocrystals on Si," *Journal of Crystal Growth*, vol. 269, no. 2–4, pp. 425–431, 2004.

[25] D. M. Bagnall, Y. F. Chen, Z. Zhu, T. Yao, M. Y. Shen, and T. Goto, "High temperature excitonic stimulated emission from ZnO epitaxial layers," *Applied Physics Letters*, vol. 73, no. 8, pp. 1038–1040, 1998.

[26] P. R. Gogate and A. B. Pandit, "A review of imperative technologies for wastewater treatment I: oxidation technologies at ambient conditions," *Advances in Environmental Research*, vol. 8, no. 3-4, pp. 501–551, 2004.

[27] P. R. Gogate and A. B. Pandit, "A review of imperative technologies for wastewater treatment II: hybrid methods," *Advances in Environmental Research*, vol. 8, no. 3-4, pp. 553–597, 2004.

[28] E. Yassıtepe, H. C. Yatmaz, C. Öztürk, K. Öztürk, and C. Duran, "Photocatalytic efficiency of ZnO plates in degradation of azo dye solutions," *Journal of Photochemistry and Photobiology A*, vol. 198, no. 1, pp. 1–6, 2008.

[29] H. Kyung, J. Lee, and W. Choi, "Simultaneous and synergistic conversion of dyes and heavy metal ions in aqueous TiO_2 suspensions under visible-light illumination," *Environmental Science and Technology*, vol. 39, no. 7, pp. 2376–2382, 2005.

[30] B. Pal and M. Sharon, "Enhanced photocatalytic activity of highly porous ZnO thin films prepared by sol-gel process," *Materials Chemistry and Physics*, vol. 76, no. 1, pp. 82–87, 2002.

[31] J. H. Sun, S. Y. Dong, Y. K. Wang, and S. P. Sun, "Preparation and photocatalytic property of a novel dumbbell-shaped ZnO microcrystal photocatalyst," *Journal of Hazardous Materials*, vol. 172, no. 2-3, pp. 1520–1526, 2009.